Phase demodulation of interferograms with open or closed fringes

Mariano Rivera
Centro de Investigacion en Matematicas A.C.,
Apdo. Postal 402, Guanajuato, Gto. Mexico 36000

Abstract

Analysis of fringe patterns with partial–field and/or closed fringes is still a challenging problem that requires the development of robust methods. This paper presents a method for fringe pattern analysis with those characteristics. The method is initially introduced as a phase refinement process for computed coarse phases, as those obtained from partial–field patterns with a full-field method for open fringes analysis. Based on the phase refinement method, it is proposed a propagative scheme for phase retrieval from closed–fringe interferograms.

In our notation, an image is a regular lattice of pixels, the set of such pixels is denoted by L and the pixel position is denoted by $r = [x, y]^T$. Then a fringe pattern, g, with or without closed fringes, is modelled by

$$g_r = a_r + b_r \cos(f_r) + \eta_r, \tag{1}$$

for all $r \in T \subseteq L$; where T is the subregion that contains the observed fringe pattern, a is the background illumination component, b is the fringe contrast, f is the unknown phase and η represents additive independent noise. In general, the terms a and b are also unknown and need be estimated. If a and b have limited bandwidth, i.e. they have smooth spatial variations, then a preprocessing of the fringe pattern can reduce significantly the contribution of a, b and η in (1) [1, 2]. If such preprocess is successfully achieved, then one obtains a normalized fringe pattern: $\hat{g}_r = \hat{b}_r \cos f_r$, where $\hat{b}$ is an estimation of b. Afterwards, on can use an existing method for demodulating closed–fringe

patterns of the form $\hat{g}$, for instance the phase–tracking method (PTM)[1, 2]. More recently, Legarda et al. [3] modified the PTM for computing b and f, simultaneously. Although our formulation admits the straightforward generalization for the joint estimation of b and f, in this paper, we focus in the estimation of the phase.

The phase refinement method assumes that there are available approximations of contrast, $\hat{b}$, and phase, ψ, in the domain of interest, R (we assume in this point that $R = T$, but in general $R \subseteq T$). Such approximations can be computed using standard fringe analysis methods, for instance, the Discrete Fourier Transform based method [4] or the one reported in Ref. [5]. As it is well known, such methods introduce artifacts at the borders of the image or along phase discontinuities. So that, in order to compute the true phase, $f = \psi + \phi$, we need to estimate a residual phase, ϕ. Now, we suppose that ψ is close enough to f such that the first order Taylor series approximate very well the model, i.e.

$$E(\phi_r) \stackrel{def}{=} \hat{g}_r - \hat{b}_r(\cos\psi_r + \phi_r \sin\psi_r) \approx 0. \tag{2}$$

Therefore, we propose to compute the residual phase, ϕ, and an outlier detector field, ω, as the minimizers of the regularized half-quadratic [6, 7] cost function:

$$\begin{aligned} U_1(\phi, \omega; \psi) &= \sum_{r \in R} \omega_r^2 E^2(\phi_r) + \mu \left(1 - \omega_r\right)^2 \\ &\quad + \lambda \sum_{\langle q,r,s \rangle \in R} \left[(\phi_q + \psi_q) - 2\left(\phi_r + \psi_r\right) + (\phi_s + \psi_s)\right]^2, \end{aligned} \tag{3}$$

where $\omega_r \in [0, 1]$ is an indicator variable that weights the individual contribution of the data; λ and μ are positive parameters that control the solution smoothness and the outlier detection, respectively. We used $\lambda = 0.2$ and $\mu = 0.01$ in our experiments. The regularization term involves cliques of size 3, $\langle q, r, s \rangle$, that correspond to horizontal, vertical and diagonals pixel triads (see figure 1). Such term is, the well known, thin plate model that penalizes changes in the second derivative of the recovered phase, $\phi + \psi$.

Given an initial phase ϕ, the refined phase $\phi + \psi$ is computed with a two step method. In the first step, the residual phase, ψ, and the weight, ω, are computed by an alternated minimization of (3); i.e., U_1 is minimized with respect to (w.r.t.) ω by keeping ϕ fixed and then it is minimized w.r.t. ϕ

with ω fixed. The minimization w.r.t. ω results in the closed formula:

$$\omega_r = \mu/[\mu + E^2(\phi_r)]. \tag{4}$$

Note that $\omega_r \approx 1$ for those sites where the square error $E^2(\phi_r)$ is small with respect to μ. On the other hand, $\omega_r \approx 0$ for those pixels where the model does not fit very well the data, so that the regularization term has more control over the computation of ϕ. In the second step, the phase ψ is updated by the computed residual ϕ, i.e.: $\psi_r = \psi_r + \phi_r$. The initial phase ϕ_r is then set to $\phi_r = 0$, for all $r \in R$. These two steps are iterated until convergence, such convergence can only be guaranteed if the computed residual phase, ϕ, is small, so that: $\|\hat{g} - \hat{b}\cos\psi\| \geq \|\hat{g} - \hat{b}(\cos\psi + \phi^T \sin\psi)\| \approx \|\hat{g} - \hat{b}\cos(\psi + \phi)\| \geq 0$ is satisfied in each iteration.

The performance of the phase refinement method is demonstrated by the experiment illustrated by figure 2. Panel 2–(a) shows an original fringe pattern of a progressive lens generated with a Moire deflectometry setup. Panel 2–(b) shows the wrapped phase computed with the Fourier method[4]. The region of interest and the wrapped refined phase are shown in panels Panel 2–(d) and 2–(c), respectively. Figure 3 shows a detail of the results in figure 2. Note that the original wrapped phase, panel 3–(a), is distorted by a border effect; such defect is corrected in the refined phase, panel 3–(c).

Now, we extend the refinement phase method for analyzing closed–fringe interferograms. Initially, the seed phase, ψ, is available for a small compact region, R, of the interferogram (note that $R \subset T$). Then we define the region S that contains the pixels located in a narrow band (with width defined by d) around R:

$$S = \{s \in T \mid s \notin R, r \in R, \|r - s\| < d\}. \tag{5}$$

We used $d = 2$ in all the experiments. The initial phase ψ in R can be computed with a method for opened–fringe patterns in a small region with such characteristics. Once the initial conditions are established (ψ, $\phi = 0$, R and S), we compute and propagate the phase using again an iterative strategy of two steps. In the first step, we refine of the phase $\psi + \phi$ in R. Then, we grow R in, at least, one pixel in the second step. The phase refinement is achieved using the previously presented method [based on (3)]. As it is known, PTM[1, 2, 3] may produce a wrong phase due to an unsuccessful normalization of the fringe pattern. In our approach, the grown pixels are chosen such that they minimize the risk of growing a wrong phase. Our growing phase strategy is detailed below.

Once the step of phase refinement is performed, we proceed to grow the region R. First, ψ is extrapolated to those pixels in S by minimizing a cost function,

$$U_2(\psi) = \sum_{\langle q,r,s\rangle:\{q,r,s\}\cap S\neq\emptyset} (\psi_q - 2\psi_r + \psi_s)^2 , \tag{6}$$

that promotes an extrapolation with constant slope and keeps fixed the values of ψ in R. Afterwards, the region R is grown by moving some pixels from S (at least one). The selection of a candidate pixel, $r \in S$ to be included in R, is done taking into account: a) the confidence of the extrapolated phase, b) the number of its neighbor pixels in R and their confidence and finally c) R is grown preferably along the fringes (i.e. the extrapolated phase is almost constant). In order to implement such constraints, we compute a "confidence measure", $\hat{\omega} \in [0, 1]$, by minimizing the cost function:

$$U_3(\hat{\omega}) = \sum_{r\in S}\left\{\hat{\omega}_r^2 E^2(\psi_r) + \mu(1-\hat{\omega}_r)^2 + \hat{\lambda}\sum_{s\in N_r} b_{rs}(\hat{\omega}_r - \hat{\omega}_s)^2\right\} \tag{7}$$

w.r.t. $\hat{\omega}$ by keeping fixed ψ and ϕ; where $N_r = \{s \mid s \in R \cup S, |r-s| < 2\}$ is the set of first eight neighbor pixels to r, $b_{rs} \in [0, 1]$ is a weight factor that measures the alignment of the pixel pair $\langle r, s\rangle$ with the local fringe and $\hat{\lambda}$ is a positive regularization parameter. The third term in (7) produces an anisotropic smoothing of $\hat{\omega}$ along the fringes. The weights, b_{rs}, are directly computed from the fringe pattern with $b_{rs} = \exp[-(r-s)^T J_r (r-s)]$, where

$$J = \mathrm{trace}(\tau\tau^T)I - \tau\tau^T, \tag{8}$$

is the local inertia tensor; with $\tau \stackrel{def}{=} [\hat{g}_{x\sigma}, \hat{g}_{y\sigma}]^T$, where $\hat{g}_{l\sigma}$ denotes the l–directional derivative smoothed with a Gaussian kernel (defined by σ) and I is the identity matrix. Note that for $\hat{\lambda} = 0$, the minimizer (7) corresponds to (4). Next, we effectively grow the region, R, where the phase can be computed by including the immediate neighbor pixels with high confidence. The smoothing of $\hat{\omega}$ and a constraint on the support of grown pixels promote smooth wavefronts and avoid the propagation to be trapped in local minima. As saddle and stationary points may induce the algorithm to produce a wrong phase, we implement a scanning strategy that leaves such problematic sites for the last, once the surrounding pixels have been demodulated. This scanning strategy is based on the assumption that the fringe patterns are locally monochromatic: just one frequency is present in a small region.

That is, the fringe patterns have a well defined local structure: small directional derivatives along the fringes and large ones across them, except in problematic sites. This growing is implemented as follows:

$$R = R \cup \{r \in S \mid c_r \cdot \hat{\omega}_r > \theta, \mathrm{card}(N_r \cap R) \geq 2\}, \tag{9}$$

where $c_r = (\lambda_{1r} - \lambda_{2r}) \,/\, (\lambda_{1r} + \lambda_{2r})$ is the local coherency that can be understood as a normalization of $\|\nabla f_r\|$; $\lambda_1 \geq \lambda_2$ are the eigenvalues of the inertia tensor, J, defined in (8) and the cardinality operator, $\mathrm{card}(\cdot)$, returns the number of elements in a set. Then, a pixel is grown if at least 2 neighboring pixels are in R (we constrained to have at least 3 neighbor in R) and its weighted confidence, $c_r \cdot \hat{\omega}_r$ pass a threshold, θ; if no pixel pass the threshold, then the one with largest $c_r \cdot \hat{\omega}_r$ is selected. The growing of R completes an iteration of wavefront propagation. The iterations continue until the phase is estimated in the region of interest: $R = T$.

Figure 4 shows the result of an experiment designed to illustrate the performance of the closed fringe analysis method. Panel 4–(a) shows the normalized fringe pattern of a real ESPI image. The fringe pattern shows the relative deformation of a steel plate when a thermal stress is applied. For illustration purposes, we show in panel 4–(b) plots of the gray level of the fringes. These plots corresponds to the row (top) and the column (bottom) that crossing at the minimum phase (fringe center). Panel 4–(c) shows the binarization of the fringes. As one can see, the normalization process is not successfully achieved as is appreciated in the figure and the fringes are not correctly distinguished. Therefore, a scanning strategy that follow fringes will compute a wrong phase. However, our method estimates the right phase in spite of the fact that we set $\hat{b} = 1$ in the whole domain. Panel 4–(d) shows the computed coherency map that defines the local threshold in (9). Panel 4–(e) shows the computed phase with the proposed method and the rewrapped phase is shown in panel 4–(f). It is important to note that, in the closed fringe analysis method, the phase refinement step can be performed in a narrow band close to the border between R and S (we use a band 3 pixels wide) with a subsequent reduction of the computational time.

We presented a phase refinement method that improves phase computed, initially, from a fringe pattern with discontinuities or incomplete domains. We generalized this phase refinement method in order estimate the phase from closed fringe patterns. This generalization is based on a successive growth of the region of phase refinement. The method has shown in real ex-

periments to be robust for analyzing fringes with spatial variable illumination conditions (see experiment of figure 4).

The author thanks to J.L. Marroquin for his comments that improved the quality of the paper. This work was partially supported by CONACYT (Mexico) under grant P40722Y1. The author's email is mrivera@cimat.mx.

References

[1] M. Servin, J.L. Marroquin, F.J. Cuevas, J. Opt. Soc. Am. A, 18, 689 (2001).

[2] M. Servin , J.L. Marroquin and J.A. Quiroga, J. Opt. Soc. Am. A, 21, 411 (2004).

[3] R. Legarda–Saenz, W. Osten and W. Jüptner, Appl. Opt. 41, 5519 (2002).

[4] M. Takeda, H. Ina and S. Kobayashi, J. Opt. Soc. Am. A, 4, 156 (1982).

[5] K. H. Womack, Opt. Eng. 23, 391 (1984).

[6] M. Rivera and J.L. Marroquin, Image Vision Comput. 21, 345 (2003).

[7] M. Rivera and J.L. Marroquin, Opt. Lett. 29, 504 (2004).

Complete References

1. M. Servin, J.L. Marroquin, F.J. Cuevas, "Fringe–follower regularized phase tracker for demodulation of closed–fringes interferograms," J. Opt. Soc. Am. A, 18, 3, 689–695 (2001).

2. M. Servin , J.L. Marroquin and J.A. Quiroga, "Regularized quadrature and phase tracking from a single closed-fringe interferogram," J. Opt. Soc. Am. A, 21, 411–419 (2004)

3. R. Legarda–Saenz, W. Osten and W. Jptner, "Improvement of the Regularized Phase Tracking Technique for the Processing of Nonnormalized Fringe Patterns ", Appl, Opt. 41, 5519–5526 (2002).

4. M. Takeda, H. Ina and S. Kobayashi, "Fourier–transform method of fringe–pattern analysis for computer–based topography and interferometry," J. Opt. Soc. Am. A, 4, 156–160 (1982).

5. K. H. Womack,"Interferometric phase measurement using spatial synchronous detection," Opt. Eng. 23, 391-395 (1984).

6. M. Rivera and J.L. Marroquin, " Half–quadratic cost functions with granularity control," Image Vision Comput. 21, 345(2003).

7. M. Rivera and J.L. Marroquin, "Half–quadratic cost functions for phase unwrapping," Opt. Lett. 29, 504–506 (2004).

Figure Captions

Figure 1. Cliques with triads of pixels $\langle q, r, s \rangle$.

Figure 2. Phase refinement. (a) Fringe pattern. (b) Approximated phase. (c) Mask. (d) Computed refined phase. The phases in (b) and (d) are rewrapped for display purposes.

Figure 3. Details of the phase refinement, the illustrated region corresponds to a rectangular region (80×80 pixels) located at the left and button of the panels 2-b, 2-c and 2-d, respectively. (a) Approximated phase. (b) Mask. (d) Refined phase.

Figure 4. Closed fringe analysis. (a) Fringe pattern. (b) Gray scale plot of the row (top) and the column (bottom) that crossing at the fringe center. (c) Binary map of fringes. (d) Coherency map. (e) Computed phase. (f) Rewrapped phase, for display purposes.

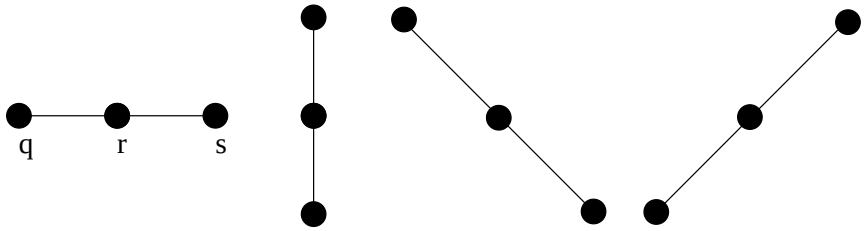

Figure 1:

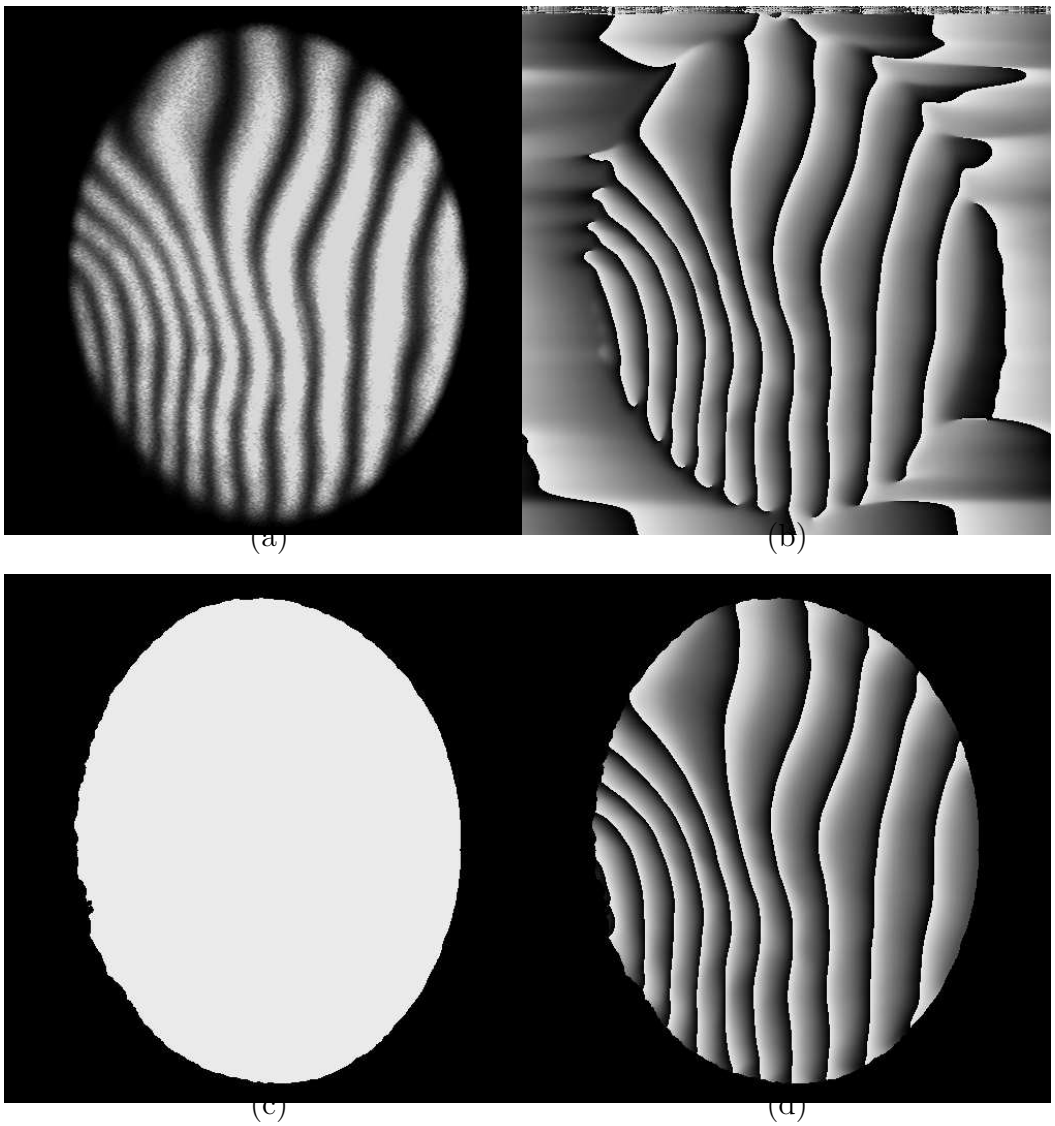

Figure 2:

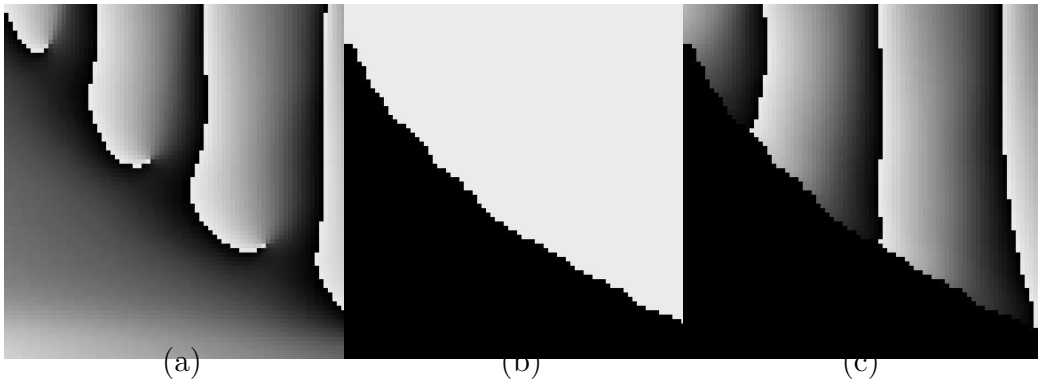

(a) (b) (c)

Figure 3:

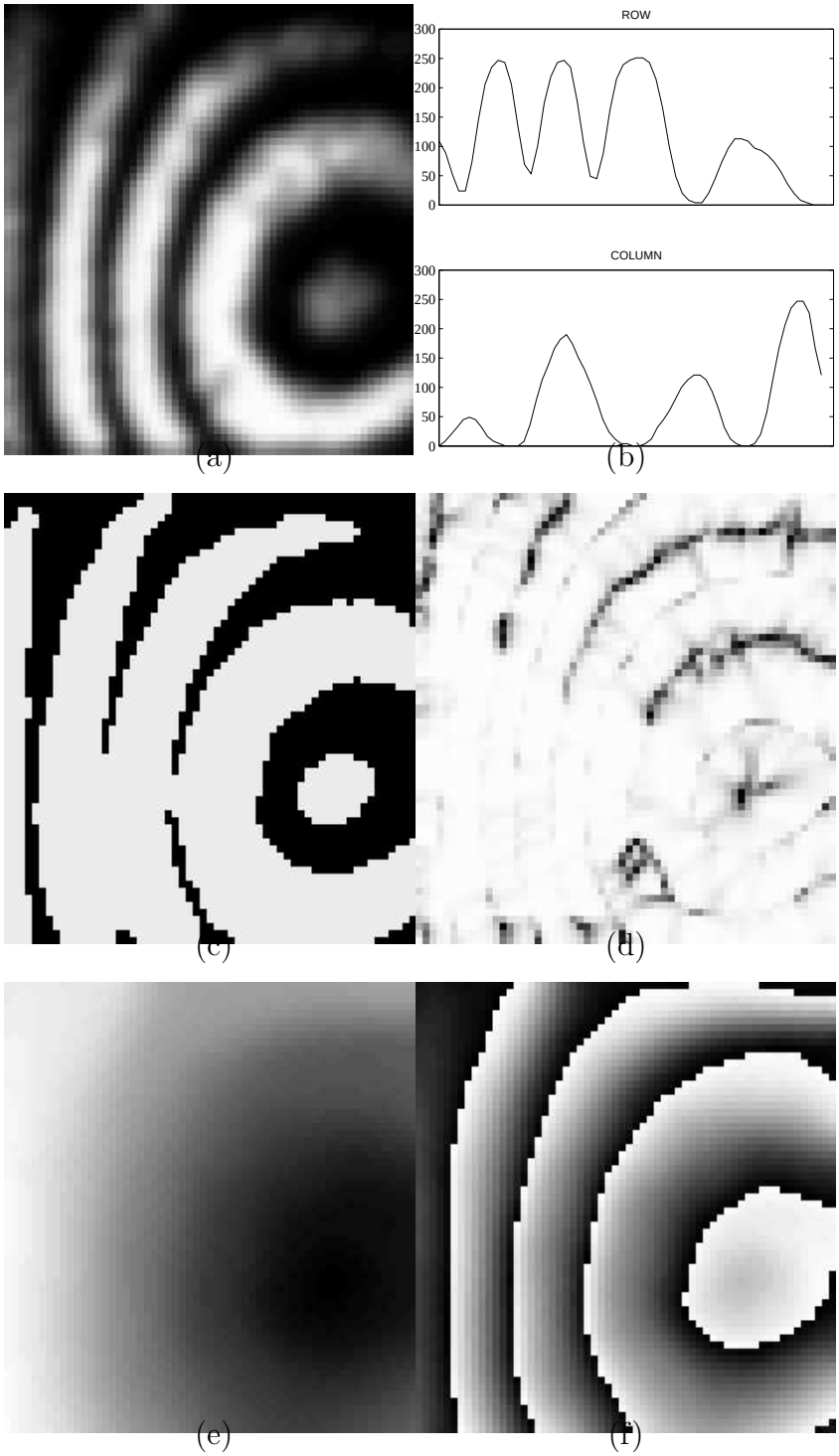
ROW
300
250
200
150
100
50
0
COLUMN
300
250
200
150
100
50
0
(a)
(b)
(c)
(d)
(e)
(f)

Figure 4: